ulm university universität
uulm

Fakultät für Naturwissenschaften

Institute of Theoretical Physics

Title of the work

Bachelor Thesis

Submitted by:
Jan Bulling
jan.bulling@uni-ulm.de
1109395

Supervised by:
Marit O. E. Steiner, Julen S. Pedernales, Martin B. Plenio

Abstract

Contents

1 Introduction **4**
1.1 Feynman's Gedankenexperiment 4

2 A first look **5**
2.1 Time evolution under a gravitational potential 9
2.2 Entanglement measures 10
2.3 Issues with the experimental procedure 14

3 Casimir effect **15**
3.1 Proximity force approximation 15
3.2 Imperfect plate and spheres 18
3.3 Casimir forces between a conducting plate and a dielectric sphere 18
3.3.1 Polarizability of a dielectric sphere 18

4 The shield **20**

5 The optimal setup **21**
5.1 Orientation 21

Bibliography **23**

A TITLE TO BE DONE **26**
A.1 Evolution under a gravitational Hamiltonian 26
A.1.1 Using time dependent perturbation theory 26
A.1.2 Using an exact time evolution 27
A.2 Exemplary calculation of E_N 27

1 Introduction

1.1 Feynman's Gedankenexperiment

2 A first look

Testing the quantum nature of gravity is no easy task and many proposals seek to detect gravitationally induced entanglement between two masses [1]!!!CITATIONS!!! as a form of proof. For all these proposals, gravity is assumed to be mediated by a gravitational field. During a time evolution, this field (like any other external field) can only make local operations (LO) on the states of the test masses. If gravity is now assumed to behave classically, the propagation between the masses can be described by a classical communication (CC) channel [1, 2]. These LOCC operations however cannot turn an initial unentangled state into an entangled one [3, 4]. It immediately follows, that if one measures the involved masses to be entangled after some after a mutual gravitational interaction, gravity necessarily has to be quantum in some way. It is important to note, that the opposite of this statement is not true. Measuring unentangled masses does not directly imply a classical gravitational field. This can be seen by considering operations that are non-LOCC and also produce unentangled states like for example the swap operation $|\psi\rangle_A |\phi\rangle_B \to |\phi\rangle_A |\psi\rangle_B$. This operations obviously can't induce entanglement to initially unentangled states, but requires the perfect exchange of quantum information between the states - which is not possible using classical communication alone. In other words: If one prepares masses initially in a pure product state and measures *any* state which cannot be obtained by LOCC-operations after some final time evolution, it is impossible for gravity to behave classical. One can even go so far and define the term ***quantum gravity*** as any interaction mediated by gravity that cannot be described by LOCC operations alone [2].

A plausible and logical arising idea for an experiment to test for gravitational induced entanglement - which is, as a reminder, enough to require gravity to be quantum - is described in this chapter. The idea requires the generation of coherent delocalized quantum superpositions of massive objects either as so-called Schrödinger-cat states or squeezed gaussian states [1, 5]. Theses masses are brought close enough together for gravity to have a measurable effect. The distances between different parts of the spatial superpositions must have different distances to the delocalized second mass. As a result - and of course *if gravity behaves quantum* - the states should get entangled. To see this, consider the ideal simplification of a real experimental setup where two bodies with mass m are trapped in an harmonic potential wall (like for example in an optical trap) with frequency ω separated by a distance d. The local Hamiltonian of the system is given by

$$\hat{H}_0 = \sum_{i=1,2} \frac{\hat{p}_i^2}{2m} + \frac{1}{2} m\omega^2 \hat{x}_i^2 \tag{2.1}$$

where $\hat{x}$ and $\hat{p}$ are the position and momentum operators satisfying the canonical com-

mutation relation $[\hat{x}_i, \hat{p}_j] = i\hbar\delta_{ij}$. For now, all non-gravitational interactions between the masses have been ignored. In the low energy regime, where the energy transfer during a process is far below the Planck scale $m_p c^2 \sim 10^{19}\,\mathrm{GeV}$, gravity can be traded as an effective field theory with tools available similar to those for the electromagnetic field and QED [6]. In the non-relativistic limit $v \ll c$, the gravitational interaction can be described by a Newtonian $1/r$ potential acting on the center-of-mass positions, with all classical quantities are replaced by quantum operators [5–7]. Spatial superpositions lead to superpositions of the metric and consequently (in the non-relativistic limit) to a superposed Newtonian potential. The interaction Hamiltonian $\hat{H}_G$ should therefore be describable by

$$\hat{H}_G = -\frac{Gm^2}{|d - \hat{x}_1 + \hat{x}_2|}, \tag{2.2}$$

where $G = 6.6743 \times 10^{-11}\,\mathrm{m^3 kg^{-1} s^{-2}}$ is the gravitational constant. The separation of the masses d is chosen much larger than the extension of the delocalization (in this setup comparable to the position variance of the harmonic oscillator). This condition is realistic given that the biggest spatial delocalization is in the order of !!!SOURCES!!!. Expanding the Hamiltonian $\hat{H}_G$ to the second order for small $\hat{x}_i$, only the order $(\hat{x}_1 - \hat{x}_2)^2$ can induce entanglement. The zeroth order term is just a overall energy offset, the first order term $\propto (\hat{x}_1 - \hat{x}_2)$ as well as the terms $\hat{x}_i^2$ result only in a local interaction for each mass separately. The coupling terms $-(\hat{x}_1\hat{x}_2 + \hat{x}_2\hat{x}_1) = -2\hat{x}_1\hat{x}_2$ however are very interesting. Introducing the ladder operators, the Hamiltonian $\hat{H} = \hat{H}_0 + \hat{H}_G$ can be expressed as [6]:

$$\hat{H} = \sum_{i=1,2} \hbar\omega \hat{a}_i^\dagger \hat{a}_i - \frac{Gm^2}{d^3}\left(\sqrt{\frac{\hbar}{2m\omega}}\right)^2 \left(\hat{a}_1\hat{a}_2 + \hat{a}_1\hat{a}_2^\dagger + \hat{a}_1^\dagger\hat{a}_2 + \hat{a}_1^\dagger\hat{a}_2^\dagger\right) \tag{2.3}$$

Applying the *rotating-wave approximation*[1], the terms $\hat{a}_1\hat{a}_2 + \hat{a}_1^\dagger\hat{a}_2^\dagger$ can be dropped. Defining the coupling strength g of the interaction as $g = Gm/\omega d^3$, eq (2.3) can be rewritten as

$$\hat{H} = \sum_{i=1,2} \hbar\omega \hat{a}_i^\dagger \hat{a}_i - \hbar g\left(\hat{a}_1\hat{a}_2^\dagger + \hat{a}_1^\dagger\hat{a}_2\right). \tag{2.4}$$

Now, for simplicity and as a simple example, the evolution of the initial Fock state $|\psi(0)\rangle = |10\rangle$ is considered. The gravitational interaction H_G can be treated as a time dependent perturbation and the state evolution is given as (for calculation see appendix A.1.1) [6]

$$|\psi(t=0)\rangle = |10\rangle \xrightarrow{\text{time } t} |\psi(t)\rangle = \mathcal{N}\left(|10\rangle - igt\,|01\rangle + \mathcal{O}(g^2)\right) \tag{2.5}$$

where $\mathcal{N}$ is an appropriate normalization constant. The evolved state (2.5) is entangled and cannot be reduced into a product state of the oscillator Fock states. The entangle-

[1] This approximation is known from quantum optics, where all fast oscillating terms in the Hamiltonian can be dropped [2, 6]. In the interaction picture, the ladder operators evolve as $\hat{a}(t) = \hat{a}e^{-i\omega t}$. The terms like $\hat{a}_1(t)\hat{a}_2(t)$ oscillate with frequency 2ω whereas $\hat{a}_1^\dagger(t)\hat{a}_2(t)$ does not oscillate at all. Due to the small coupling, this approximation works very well here.

ment is very small since it is proportional to the gravitational coupling constant gt [2] but can still be measured by ???? !!!SOURCES!!!. Another interesting result, which underlines the false inference of a classical gravity from observed non-entanglement discussed above can be seen by considering the time evolution of a coherent product state $|\alpha\rangle \otimes |\beta\rangle$ where $\hat{a}\,|\alpha\rangle = \alpha\,|\alpha\rangle$. The time evolution is derived in appendix A.1.2 and results in

$$e^{-i\hat{H}t/\hbar}\left(|\alpha\rangle \otimes |\beta\rangle\right) = \left|e^{-i\omega t}\left(\alpha\cos gt - \beta\sin gt\right)\right\rangle \otimes \left|e^{-i\omega t}\left(-\alpha\sin gt + \beta\cos gt\right)\right\rangle . \quad (2.6)$$

This state is clearly a product state and thus not entangled. But for a time $t_0 = \pi/2g$ the state is effectively the swapped initial state $|\beta\rangle \otimes |\alpha\rangle$ up to a local phase. This swap operation is however, as established earlier, not possible under a LOCC protocol. Thus, even if the resulting state after time evolution under a gravitational interaction is unentangled, we can role out the classicality of gravity [2, 6]. Gravity must therefore be capable of transmitting quantum information, namely the superposition of one mass needs to be transmitted to the other mass.

Experimentally, one requires the ability to generate spatial superpositions of two massive objects with large enough coherence times. Usually the weak gravitational interaction requires coherence times in the order of $100\,\mathrm{ms} - 10\,\mathrm{s}$ for any meaningful and measurable entanglement to built up. The masses should additionally be massive enough for their gravitational effects to be measurable. These requirements impose huge experimental and engineering challenges. To contextualize: The most massive object ever put into a spatial superposition is in the order of $4 \times 10^{-23}\,\mathrm{kg}$, whereas the smallest object whose gravitational field has been measured was just below $100\,\mathrm{mg}$ [8] - a difference of 19 orders of magnitude, comparable to the difference between the mass of a car and the mass of the earth's moon. Such spatial superpositions can be created experimentally by giving the masses a spin-1/2 degree of freedom. For example a nitrogen-vacancy diamonds can be used [1], where the NV site provides the required spin of 1/2. An applied magnetic gradient functions like a "beam splitter" and creates a delocalized state. The extend of this superposition can be calculated and separations in the order of $100\,\mu\mathrm{m}$ are theoretically achievable [1]. Levitated particles in a trap or free-falling experiments isolated and shielded in a vacuum can increase environmental isolation by avoiding contact with surrounding noise. The additional forces due to the trapping potential or the gravitational acceleration can be studied in advance. For now, I assume that all required states and superpositions can be experimentally prepared.

The general and idealized problem considered is illustrated in fig. 2.1. Two massive bodies with masses M_A and M_B are initially separated by a center-to-center distance $2L$. The masses are prepared in a coherent delocalized quantum superposition Schrödinger-cat-like state in, for now, a parallel orientation as depicted in fig. 2.1. The extension of the superposition is denoted by Δx and is the same for both masses. It is important to choose the positions of the masses such that the distances between each part of the delocalized mass A and B are not always identical. Otherwise, all built up phases are

[2] The amount of entanglement can for example be measured with the later introduced *logarithmic negativity* E_N. For this state, this quantity is given as $E_N(|\psi(t)\rangle\langle\psi(t)|) \simeq 2tg/\log 2 + \mathcal{O}(g^2) \geq 0$.

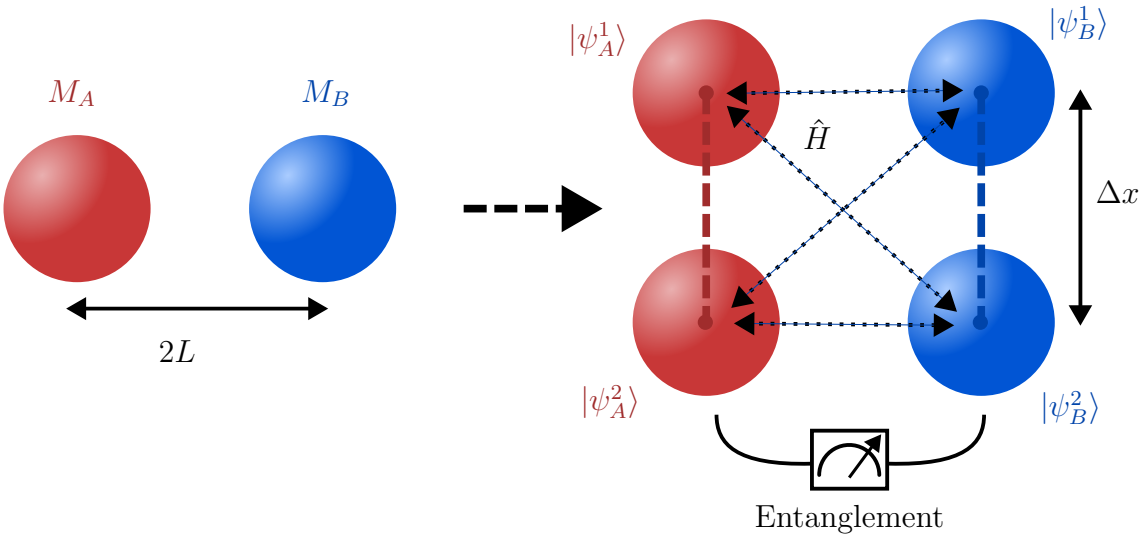

Figure 2.1: Schematic figure of the proposed experiment with two masses prepared in a spatial superposition state. The gravitational interaction $\hat{H}$ induces different phases to each of the superpositions due to the different distances between all masses. This results in measurable entanglement after some time evolution.

the same and no entanglement is observable. With the notation introduced in fig. 2.1, the initial state at $t = 0$ is given by

$$|\psi(t=0)\rangle = \frac{1}{2}\left(\left|\psi_A^1\right\rangle + \left|\psi_A^2\right\rangle\right) \otimes \left(\left|\psi_B^1\right\rangle + \left|\psi_B^2\right\rangle\right). \tag{2.7}$$

The state evolves under a Hamiltonian $\hat{H}$ and after some time the position of each mass is measured and checked for entanglement. For now I assume that all interactions expect gravity can be neglected. In reality, electromagnetic forces and Casimir-Polder interactions [9, 10] need to be considered.

As established earlier in this chapter, gravitational interaction can generate entanglement. In the time scales of the experiment, the acceleration of the masses due to the mutual gravitational interaction can be neglected. The Hamiltonian therefore only needs to include the gravitational potential

$$\hat{V} = -\frac{GM_AM_B}{\left|\hat{D}\right|} \tag{2.8}$$

where $\hat{D}$ is the distance operator between the masses. It depends on the individual positions $\hat{x}_A$ and $\hat{x}_B$. During time evolution, the different parts of the superpositions built up different local phases. I am interested in calculating, how much entanglement one can expect from this kind of interactions.

2.1 Time evolution under a gravitational potential

Proposition 2.1. *The time evolution under a static and constant Hamiltonian* $\hat{H} = \hat{V}(\hat{x}_i) = \text{const.}$ *is given by the eigenenergies of the system* $\hat{V}|n\rangle = V_n|n\rangle$ *as* $\sim e^{-iV_n t/\hbar}$.

Proof. This is a trivial statement. The time evolution is governed by the Schrödinger equation

$$i\hbar\frac{\partial}{\partial t}|\psi(t)\rangle = \hat{H}|\psi(t)\rangle . \tag{2.9}$$

The formal solution of this first order PDE is given by

$$|\psi(t)\rangle = e^{-i\hat{V}t/\hbar}|\psi(t=0)\rangle . \tag{2.10}$$

The constant (hermitian) potential operator can be expressed in the energy-eigenbasis $\{|n\rangle\}$ as $\hat{V}|n\rangle = V_n|n\rangle$. The initial state can be expressed as a superposition in the same eigenstates like $|\psi\rangle = \sum_n c_n|\psi_n\rangle$. Putting both together and using the taylor expansion of the exponential function, one arrives at the simple form

$$|\psi(t)\rangle = \sum_n e^{-i\hat{V}t/\hbar}|n\rangle\langle n|\psi\rangle = \sum_{n,k}\frac{(-i\hat{V}t/\hbar)^k}{k!}|n\rangle c_n|\psi_n\rangle \tag{2.11}$$

$$= \sum_{n,k}\frac{(-iV_n t/\hbar)^k}{k!}c_n|\psi_n\rangle = \sum_n e^{-iV_n t/\hbar}c_n|\psi_n\rangle \tag{2.12}$$

where in the second to last step $\hat{V}^k|n\rangle = \hat{V}^{k-1}\hat{V}|n\rangle = \hat{V}^{k-1}|n\rangle V_n = \cdots = V_n^k|n\rangle$ was used. □

Using the preceding proposition, the initial state eq. (2.7) can be evolved in time. The potential operator eq. (2.8) acts on every state in the $\{|\psi_A^1\rangle, |\psi_A^2\rangle\}\otimes\{|\psi_B^1\rangle, |\psi_B^2\rangle\}$ basis differently. This is because of the different distances between the states $|\psi_A^i\rangle$ and $\left|\psi_B^j\right\rangle$ for different $i,j\in\{1,2\}$. This results in phases ϕ_{ij} to be built up during time evolution according to proposition 2.1. The state $|\psi(t)\rangle$ after some time evolution is therefore given as

$$|\psi(t)\rangle = \frac{1}{2}\Big(e^{i\phi_{11}}\left|\psi_A^1\right\rangle\left|\psi_B^1\right\rangle + e^{i\phi_{12}}\left|\psi_A^1\right\rangle\left|\psi_B^2\right\rangle + e^{i\phi_{21}}\left|\psi_A^2\right\rangle\left|\psi_B^1\right\rangle + e^{i\phi_{22}}\left|\psi_A^2\right\rangle\left|\psi_B^2\right\rangle\Big), \tag{2.13}$$

where the $\otimes$ symbol was omitted. The phases are

$$\phi \equiv \phi_{11} = \phi_{22} = \frac{GM_AM_B}{2\hbar L}t \qquad \text{and} \qquad \phi_{12} = \phi_{21} = \frac{GM_AM_B}{\hbar\sqrt{4L^2+(\Delta x)^2}}t. \tag{2.14}$$

Assuming again that the superposition size Δx is much smaller than the distance L between the masses - like before in eq. (2.2) - the phases $\phi_{12} = \phi_{21}$ can be expanded and a global phase ϕ can be factored:

$$\phi_{12} = \phi_{21} \approx \frac{GM_AM_B}{\hbar}\left[\frac{1}{2L} - \frac{(\Delta x)^2}{16L^3}\right]t \equiv \phi - \Delta\phi. \tag{2.15}$$

The state eq. (2.13) can now be expressed in the form

$$|\psi(t)\rangle = e^{i\phi}\frac{1}{\sqrt{2}}\left[\left|\psi_A^1\right\rangle \otimes \frac{|\psi_B^1\rangle + e^{-i\Delta\phi}\,|\psi_B^2\rangle}{\sqrt{2}} + \left|\psi_A^2\right\rangle \otimes \frac{e^{-i\Delta\phi}\,|\psi_B^1\rangle + |\psi_B^2\rangle}{\sqrt{2}}\right], \tag{2.16}$$

where the entanglement dynamics can be directly seen. This state is entangled, if it is not representable as a product state $|\psi\rangle \neq |\psi_A\rangle \otimes |\psi_B\rangle$. That is the case, if the states containing $|\psi_B^i\rangle$ are not both equal to each other (i.e. differ only by a phase) and thus cannot be factored. The system is therefore entangled, if and only if $\Delta\phi \neq k\pi$ with integer $k \in \mathbb{Z}$.

In order to assess in a more quantitative way how entangled the state $|\psi\rangle$ is, a more sophisticated entanglement measure is needed. In the next chapter, the ***logarithmic negativity*** is motivated and introduced. In the rest of this thesis, I will repeatedly opt for this measure.

2.2 Entanglement measures

Checking whether an arbitrary state ρ is entangled or not is no easy task. In fact, this problem is known to be NP-hard [11]. A state $\rho_{AB} \in \mathcal{H}_A \otimes \mathcal{H}_B$ is called entangled, if it is ***non-separable***, that is, it cannot be expressed as a tensor product of two subsystems $\rho_A \in \mathcal{H}_A$ and $\rho_B \in \mathcal{H}_B$. In particular, it is very difficult to check if a mixed state is entangled or not. Only for specific cases - like the case of two qubits or qubit-qutrit - a simple sufficient criterion for determining separability is known: The positive partial transpose (PPT) criterion states, that if the partial transpose of the density matrix is positive ($\rho^{\Gamma_A} \geq 0$ [3]), the state ρ is separable [3, 4]. In other words, if ρ^{Γ_A} has negative eigenvalues, ρ is guaranteed to describe an entangled state. The inverse is true, if and only if the dimension of $\rho_A \otimes \rho_B$ is 2×2 or 3×2 [3] - only having non-negative eigenvalues doesn't necessarily result in an unentangled system (such states are called "bound states"). The partial transpose with respect to a subsystem i can be understood in the same way as the partial trace, where the operation (in this case the transform) is performed only on indices corresponding the subsystem ρ_i and can be interpreted as a partial time reversal. To see the necessity of the PPT criterion, consider a separable mixed state ρ, which can be generally expressed as

$$\rho = \sum p_i \rho_A^i \otimes \rho_B^i. \tag{2.17}$$

The partial transpose is in this case trivial:

$$\rho^{\Gamma_A} = \sum p_i (\rho_A^i)^T \otimes \rho_B^i. \tag{2.18}$$

Since the transpose preserves eigenvalues, the transposed subsystem A is still positive $(\rho_A^i)^T \geq 0$ and thus describes again a valid quantum state. It follows, that ρ^{Γ_A} is again

[3] A matrix is defined as positive ("positive definite"), if all eigenvalues are positive.

positive. If somehow ρ^{Γ_A} has any negative eigenvalues, this can only mean that the initial state ρ is not separable and cannot be expressed in the form of eq. (2.17) and the necessity of the criterion is shown.

For quantifying entanglement, a mathematical quantity called ***entanglement measure*** can be used. A good measure should be able to capture the essential features of entanglement. With this property, one can axiomatically state what properties such a measure $E(\rho)$ should have [3, 4]:

Monotonicity under LOCC E should not increase under local operations and classical communications. This is the most important postulate for an entanglement measure and often cited as the *only* required postulate.

Vanishing on separable states $E(\rho) = 0$ if ρ is separable

Often one finds additional properties useful like *convexity* $E(\sum p_i\rho_i) \leq \sum p_i E(\rho_i)$, (full) *additivity* $E(\rho\otimes\sigma) = E(\rho)+E(\sigma)$ or a normalization that the maximally entangled state has $E = 1$.

A function that satisfies the most important of these conditions is often called an *entanglement monotone*.

The ***negativity*** $\mathcal{N}$ is such a entanglement monotone [4] that used the PPT criterion to determine if a state is entangled or not. It is defined as

$$\mathcal{N} = \frac{\left\|\rho^{\Gamma_A}\right\|_1 - 1}{2} \tag{2.19}$$

where $\|A\|_1 = \operatorname{tr}|A| = \operatorname{tr}\sqrt{A^\dagger A}$ is the trace norm. The negativity however is not additive and a more suitable and widely used entanglement measure is the ***logarithmic negativity*** [3, 4, 12]

$$E_N(\rho) = \log_2 \left\|\rho^{\Gamma_A}\right\|_1 . \tag{2.20}$$

The monotonicity of the logarithm implies, that E_N is an entanglement monotone as well. Furthermore, for the calculations it does not matter which subsystem is transposed.

Proposition 2.2. *a) The partial transpose w.r.t. subsystem A is equal to the transposed partial transpose w.r.t. subsystem B:* $\rho^{\Gamma_A} = (\rho^{\Gamma_B})^T$. *b) The trace norms of partially transposed density operators w.r.t. any subsystem are equal:* $\left\|\rho^{\Gamma_A}\right\|_1 = \left\|\rho^{\Gamma_B}\right\|_1$.

Proof. a) A general density matrix ρ can be expressed as

$$\rho = \sum_{i,j,k,l} \rho_{ij,kl} \, |i\rangle\langle j|_A \otimes |k\rangle\langle l|_B$$

The partial transpose with respect to subsystem B is then defined as

$$\rho^{\Gamma_B} \equiv \sum_{i,j,k,l} \rho_{ij,kl} \, |i\rangle\langle j|_A \otimes \left(|k\rangle\langle l|_B\right)^T = \sum_{i,j,k,l} c_{ij,kl} \, |i\rangle\langle j|_A \otimes |l\rangle\langle k|_B$$

The complete transpose of this is

$$(\rho^{\Gamma_B})^T = \sum_{i,j,k,l} \rho_{ij,kl} \left(|i\rangle\langle j|_A\right)^T \otimes \left(|l\rangle\langle k|_B\right)^T = \sum_{i,j,k,l} c_{ij,kl} \, |j\rangle\langle i|_A \otimes |k\rangle\langle l|_B \equiv \rho^{\Gamma_A}$$

b) Clear by a) and by using lemma 2.1 and the fact that the eigenvalues of a square matrix A and A^T are equal. □

The logarithmic negativity is very easy to calculate compared to other entanglement measures. It is enough to compute the square root of the eigenvalues of $(\rho^\Gamma)^\dagger \rho^\Gamma$ or the absolute sum of the eigenvalues of ρ^Γ. For practical and numeric calculations it is often more easy and stable to take a single eigenvalue than the need to compute the sum of multiple. For all numerical calculations in this thesis, I therefore opt for an alternative way to compute the logarithmic negativity.

Lemma 2.1. *The trace norm* $\|A\|_1 \equiv \operatorname{tr}\sqrt{A^\dagger A}$ *of a hermitian matrix* A *is equal to the sum of the absolute eigenvalues of* A*.*

Proof. This can be immediately seen by the spectral theorem:

$$\operatorname{tr}\sqrt{A^\dagger A} = \operatorname{tr}\sqrt{A^2} = \operatorname{tr}\left\{U\sqrt{\operatorname{diag}(\lambda_1, \dots)^2}U^\dagger\right\} = \sum_i \sqrt{\lambda_i^2} = \sum_i |\lambda_i| \,.$$

□

Proposition 2.3. *The negativity eq.* (2.19) *is given as the absolute sum of all negative eigenvalues of* ρ^Γ*:*

$$\mathcal{N}(\rho) \equiv \frac{\left\|\rho^\Gamma\right\|_1 - 1}{2} = \left|\sum_{\lambda_i<0} \lambda_i\right| . \tag{2.21}$$

Proof. The proof is in parts given by Vidal [13]. It is known that the density matrix is hermitian: $\rho = \rho^\dagger$. Using lemma 2.1, the trace norm of the density matrix is is given as $\|\rho\|_1 = \sum \lambda_i = \operatorname{tr}\rho = 1$. The partial transpose ρ^Γ obviously also satisfies $\operatorname{tr}\rho^\Gamma = 1$ but might have negative eigenvalues. Since ρ^Γ is still hermitian, the trace norm is given by

$$\left\|\rho^\Gamma\right\|_1 = \sum_i |\lambda_i| = \sum_{\lambda_i \geq 0} \lambda_i + \sum_{\lambda_i<0} |\lambda_i| = \sum_i \lambda_i + 2\sum_{\lambda_i<0} |\lambda_i| = 1 + 2\sum_{\lambda_i<0} |\lambda_i| \,,$$

where in the last step $\sum \lambda_i = \operatorname{tr}\rho^\Gamma = 1$ was used. The negativity can be defined as $\mathcal{N}(\rho) = \left|\sum_{\lambda_i<0} \lambda_i\right|$ and the statement is shown. □

Remark. The PPT criterion states, that if ρ^Γ has negative eigenvalues, the state ρ is entangled. The negativity uses this criterion for a quantification of entanglement. This proposition makes sense of the name *negativity*.

Calculating the logarithmic negativity of the evolved state eq. (2.13), it is possible to quantify how the entanglement behaves in time. A straight forward computation following the calculation methods established above yields (for detailed calculations see appendix A.2)

$$E_N(|\psi(t)\rangle\langle\psi(t)|) = \log_2(1 + |\sin\Delta\phi|)\,. \tag{2.22}$$

It is interesting to see, that the maximum entanglement $E_N = 1$ is reached for $\Delta\phi = 2\pi k \pm \pi/2$, $k \in \mathbb{Z}$ and no entanglement ($E_N = 0$) is measurable for $\Delta\phi = k\pi$. This result aligns with the previous observations by demanding that the evolved state eq. (2.13) is separable. The complete entanglement dynamics are shown in fig. 2.2. The time

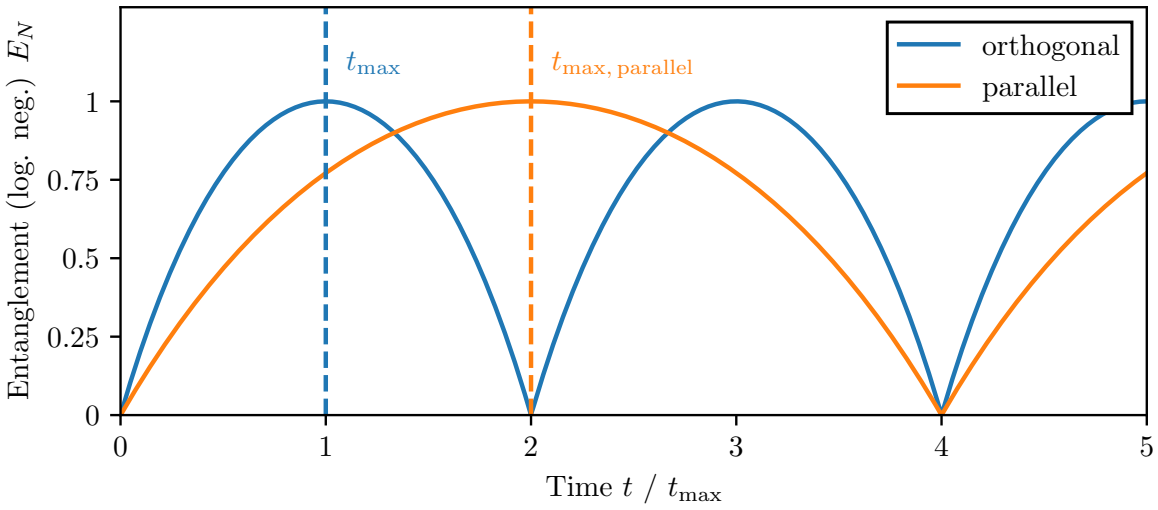

Figure 2.2: Entanglement dynamics quantified by the logarithmic negativity for two different orientations of the spatial superpositions. The parallel orientation was considered in this chapter (see eq. (2.22)), the "orhtogonal" one in Ref. [5]. The time of maximum entanglement $t_{\max}$ for the orthogonal configuration is reached after $t_{\max} = 4\pi\hbar L^3/(GM_AM_B\Delta x^2) \simeq 129\,\mathrm{ms}$.

$t_{\max,\,\mathrm{parallel}}$ at which the entanglement is maximal (for the first time) can be calculated by using the definition of $\Delta\phi$ from eq. (2.15) as

$$t_{\max,\,\mathrm{parallel}} = \frac{8\pi L^3\hbar}{GM_AM_B(\Delta x)^2}. \tag{2.23}$$

In fig. 2.2 the entanglement dynamics for a different orientation considered in Ref. [5] is also shown. There, the superpositions are aligned in the same line as the direct connection between the masses ("orthogonal" to the parallel configuration before), maximizing the differences in distances between them and thus creating entanglement faster. This expected behavior can be well seen in fig. 2.2: The time $t_{\max}$ until the maximum entanglement is reached, is precisely by a factor of 2 faster than in the here considered parallel configuration [5]. For a practical experiment, this suggests that using the orthogonal orientation could be beneficial and would require shorter coherence times for

the superpositions. To give an estimate, consider two identical silica spheres with a density of $\rho = 2648\,\mathrm{kg/m^3}$ with a radius of $R = 10^{-5}\,\mathrm{m}$, a separation of $2L = 4R$ and a superposition size $\Delta x = 100\,\mathrm{nm}$ (which is realistic considering theoretical sizes of up to micrometers [1]), the maximum entanglement is reached after about $t_{\max} \approx 129\,\mathrm{ms}$ which is a quite long coherence time and challenging experimentally.

2.3 Issues with the experimental procedure

Additional effects: - Casimir forces entangle as well - Coulomb forces

-¿ solution: conducting faraday shield, UV discharge [14]

How to measure? Many measurements are necessary -¿ Entanglement witness? Measure density directly -¿ Small variations for each measurement in angle of the superposition and in distance to the newly introduced shield

3 Casimir effect

General introduction and comparison with retarded van der Waals forces

$$F_{\text{Casimir}} = -\frac{\hbar c \pi^2}{240 L^4} A \tag{3.1}$$

$$V_{\text{Casimir}} = \frac{\hbar c \pi^2}{720 L^3} A \tag{3.2}$$

Lifshitz:

$$F_{\text{DD}} = \frac{\hbar c \pi^2}{240 L^4} \left(\frac{\varepsilon_r - 1}{\varepsilon_r + 1} \right)^2 \varphi(\varepsilon_r) \tag{3.3}$$

$$F_{\text{DM}} = \frac{\hbar c \pi^2}{240 L^4} \frac{\varepsilon_r - 1}{\varepsilon_r + 1} \varphi(\varepsilon_r) \tag{3.4}$$

The numeric function φ is shown in fig. 3.1.

3.1 Proximity force approximation

The Casimir-Polder force cannot be calculated easily for different shapes. There even exists no analytic expression for the simple (and for this thesis relevant) plate-sphere geometry for all ratios L/R and plate-sphere separations. For a general shape, even the sign of the force, i.e. whether it is attractive or repulsive, is often unknown. Fortunately, approximation methods exist and in particular the ***proximity-force-approximation (PFA)*** can be calculated very easily [15–17]. The PFA is only valid for small separations ($L/R \approx 1$) between the considered smooth bodies. The idea of this approximation is to divide the surfaces of the two bodies into infinitesimal small parallel plates with area $\mathrm{d}A$ and summing over the forces $\mathrm{d}F$ (or the Casimir-energy $\mathrm{d}E$) between them (see fig. 3.2):

$$E_{\text{PFA}} = \iint_A \mathrm{d}A \, \frac{E_{\text{plate-plate}}}{A} \tag{3.5}$$

where for the casimir energy per unit area $E_{\text{plate-plate}}/A$ either eq. (3.2) or any of the Lifshitz equations (3.3), (3.4) can be chosen. For the following calculations, it is important to distinguish between the distance between the plates center and the spheres center L (like used before) and the edge-to-edge distance $\mathscr{L} = L - R$.

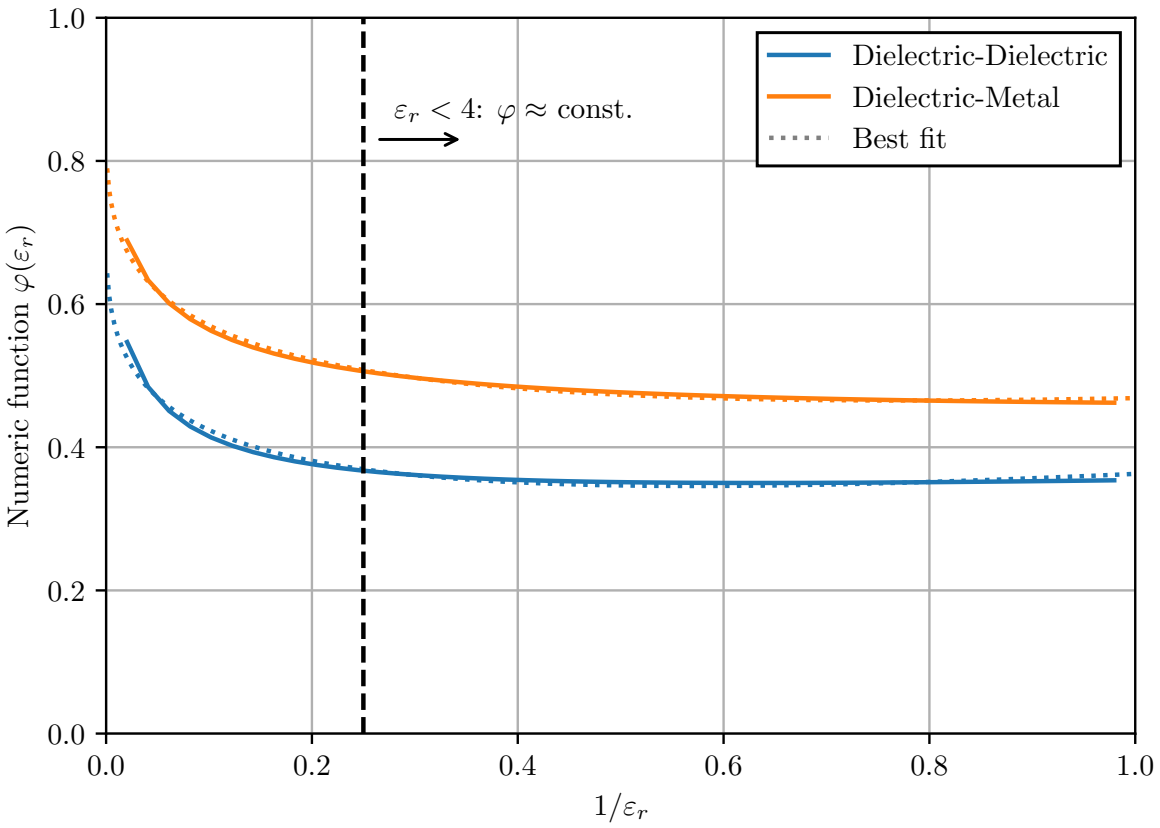

Figure 3.1: Numeric casimir interaction $\varphi(\epsilon_r)$ between **(blue)** two dielectric plates and **(orange)** a dielectric and a conductor.

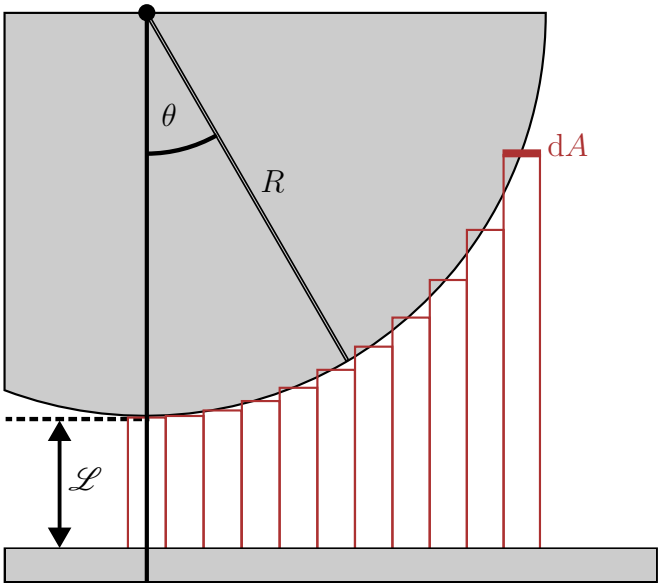

Figure 3.2: In the proximity force approximation the sphere is divided into infinitesimal plane areas $\mathrm{d}A$ which all exert a force $\mathrm{d}F$ according to eq. (3.1). All the contributions are added up together.

The problem with this approximation is, that it is ambiguous, what surface the area element $\mathrm{d}A$ represents. For the plate-sphere geometry, the element can be either chosen tangential to the sphere or parallel to the plate (or in theory any other fictitious surface somewhere in between) [17]. For the plate-sphere geometry, in the limit of the validity of the PFA $\mathscr{L} \ll R$ both methods yield the same result. For the following calculations, I choose $\mathrm{d}A$ parallel to the plate and the area can be parameterized with $r \in [0, R]$ and $\varphi \in [0, 2\pi]$ resulting in a distance z between the infinitesimal area elements $z(r) = \mathscr{L} + R - \sqrt{R^2 - r^2}$ [4]. The PFA eq. (3.5) then yields for a dielectric sphere against a perfectly conducting plate

$$E_{\text{plate-sphere}} = -\frac{\hbar c \pi^2}{720}\left(\frac{\varepsilon_r - 1}{\varepsilon_r + 1}\right)\varphi(\varepsilon_r)\int_0^R \mathrm{d}r \int_0^{2\pi} r\mathrm{d}\varphi \frac{1}{z(r)^3} \tag{3.6}$$

$$= -\frac{\hbar c \pi^3}{360}\left(\frac{\varepsilon_r - 1}{\varepsilon_r + 1}\right)\varphi(\varepsilon_r)\frac{R^2}{2\mathscr{L}^2(R + \mathscr{L})} \tag{3.7}$$

$$\approx -\frac{\hbar c \pi^3}{720}\left(\frac{\varepsilon_r - 1}{\varepsilon_r + 1}\right)\varphi(\varepsilon_r)\frac{R}{\mathscr{L}^2} \tag{3.8}$$

[4] Taking $\mathrm{d}A$ tangential to the sphere, it can be parameterized with $\theta \in [0, \pi/2]$ and $\varphi \in [0, 2\pi]$ resulting in $z(\theta) = \mathscr{L} + R - R\cos\theta$. The PFA eq. (3.5) yields with $\mathrm{d}A = R^2 \sin\theta \mathrm{d}\theta\mathrm{d}\varphi$ the result $\propto \frac{\pi R^2(R+2\mathscr{L})}{\mathscr{L}^2(R+\mathscr{L})^2}$ which in the limit of $\mathscr{L} \ll R$ results in the same expression as eq. (3.8).

3.2 Imperfect plate and spheres

Python numerical approach, gaussian modes (vibration modes of a spherical plane), perlin noise

3.3 Casimir forces between a conducting plate and a dielectric sphere

3.3.1 Polarizability of a dielectric sphere

The polarizability α is defined via

$$\mathbf{E}_\infty \alpha = \mathbf{p}, \tag{3.9}$$

where $\mathbf{p}$ is the induced dipole moment and $\mathbf{E}_\infty$ is the external electric field that induces the dipole moment. For a linear and uniform dielectric, it is given as $\mathbf{p} = \mathcal{V}\varepsilon_0(\varepsilon_r - 1)\mathbf{E}_{\text{in}}$ [18, p. 220-226]. Here, $\mathcal{V}$ is the volume of the object and $\mathbf{E}_{\text{in}}$ is the electric field inside the dielectric. The electrostatic boundary conditions for the problem are given by

$$V_{\text{in}}\Big|_{r=R} = V_{\text{out}}\Big|_{r=R} \quad \text{and} \quad \varepsilon_r\varepsilon_0 \frac{\partial V_{\text{in}}}{\partial r}\bigg|_{r=R} = \varepsilon_0 \frac{\partial V_{\text{out}}}{\partial r}\bigg|_{r=R} \tag{3.10}$$

and the electric potential outside of the sphere at $r \to \infty$ should be equal to the external dipole-inducing field $V_{\text{out}}|_{r\to\infty} = -\mathbf{E}_\infty \cdot \mathbf{r} = -E_\infty r\cos\theta$. The electric potential inside and outside the sphere can be calculated using the spherical decomposition of the general electric potential $V \propto 1/|\mathbf{r} - \mathbf{r}'|$ into Legendre Polynomials P_l [18, p. 188-190]:

$$V_{\text{in}}(r,\theta) = -E_\infty r\cos\theta + \sum_{l=0}^{\infty} A_l r^l P_l(\cos\theta), \tag{3.11}$$

$$V_{\text{out}}(r,\theta) = -E_\infty r\cos\theta + \sum_{l=0}^{\infty} \frac{B_l}{r^{l+1}} P_l(\cos\theta). \tag{3.12}$$

Applying both boundary conditions, it follows that [18, p. 249-251]

$$\begin{cases} A_l = B_l = 0 & \text{for } l \neq 1, \\ A_1 = -\frac{3}{\varepsilon_r+2}E_\infty, \quad B_1 = \frac{\varepsilon_r-1}{\varepsilon_r+2}R^3 E_\infty \end{cases} \tag{3.13}$$

and the resulting homogenous electric field $\mathbf{E}_{\text{in}} = -\nabla V_{\text{in}}$ inside the sphere is given as

$$\mathbf{E}_{\text{in}} = \frac{3}{\varepsilon_r + 2}\mathbf{E}_\infty. \tag{3.14}$$

The field is shown on the right in fig. 3.3.The polarizability α of the sphere can be now be determined to

$$\alpha_{\text{sphere}} = 4\pi\varepsilon_0 R^3 \left(\frac{\varepsilon_r - 1}{\varepsilon_r + 2}\right). \tag{3.15}$$

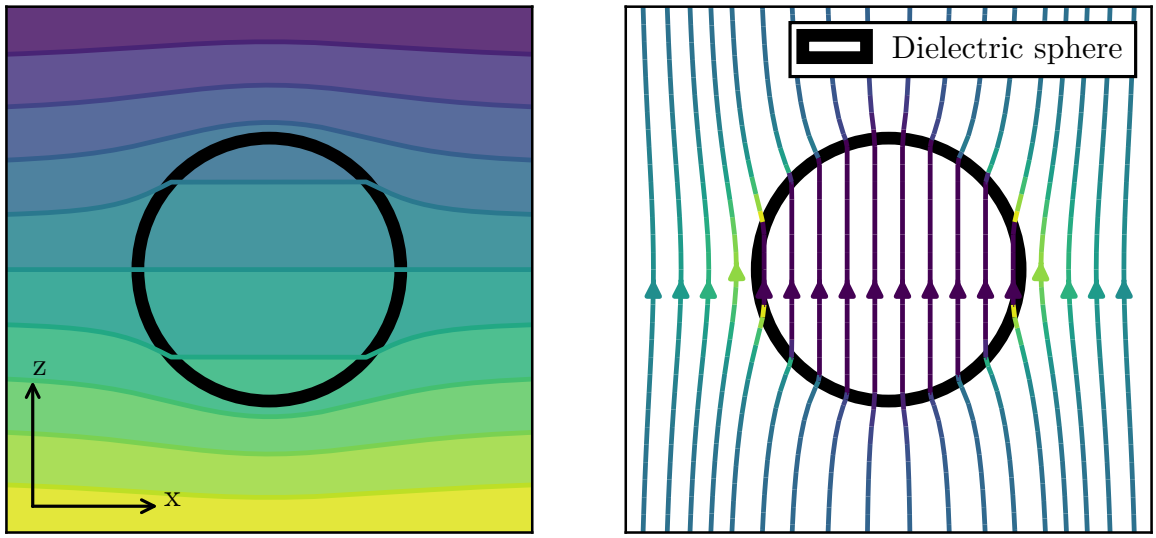

Figure 3.3: left: Electric potential V of a dielectric sphere in a external electric field $\mathbf{E}_\infty \parallel \mathbf{e_z}$. **right:** The corresponding electric field lines inside and outside the dielectric sphere.

4 The shield

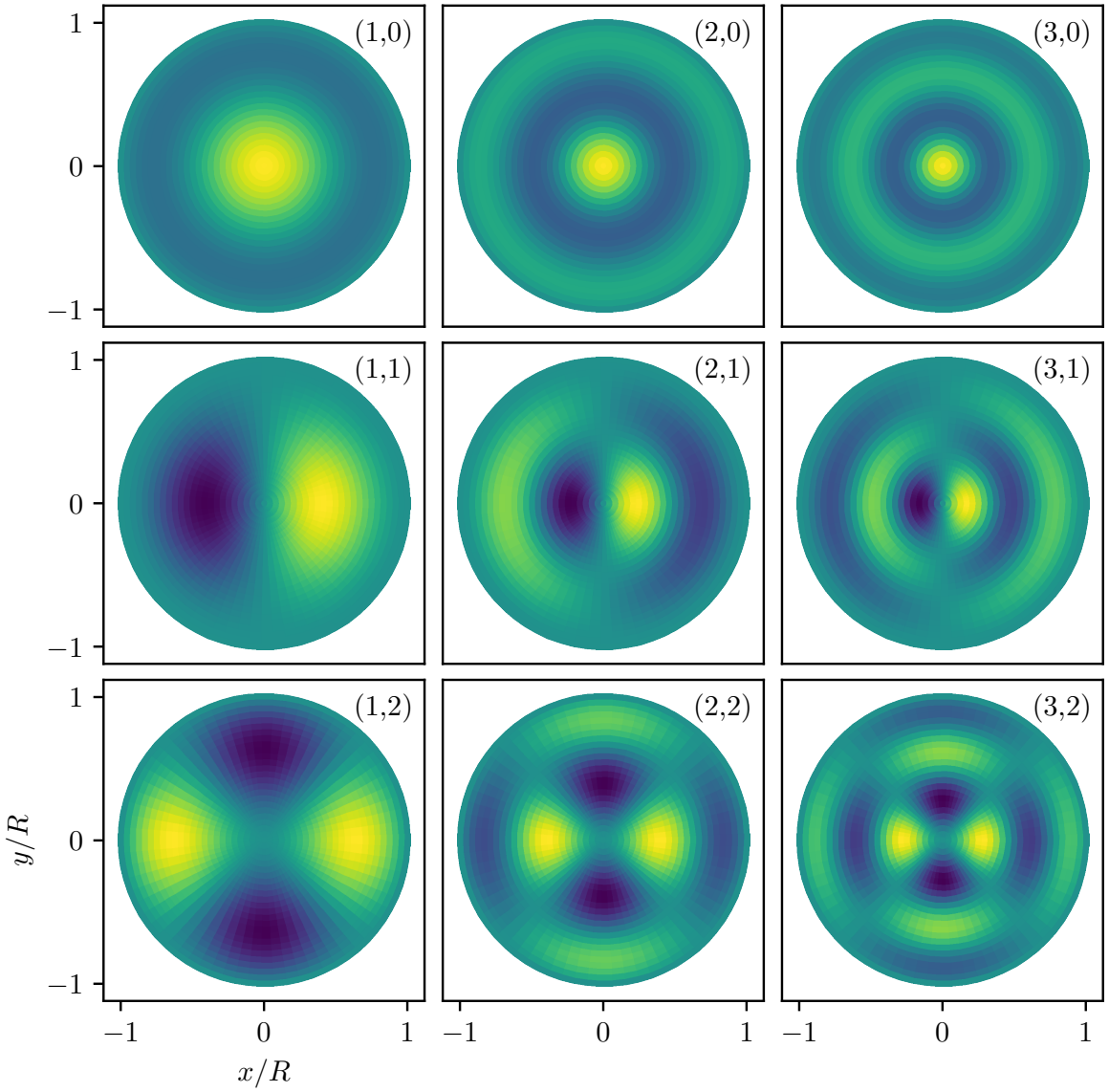

Figure 4.1: Vibrational modes of a spherical plate fixed at the edge with $R/d = 1000$.

Gravitational effect of the shield is neglectable PROOF:

5 The optimal setup

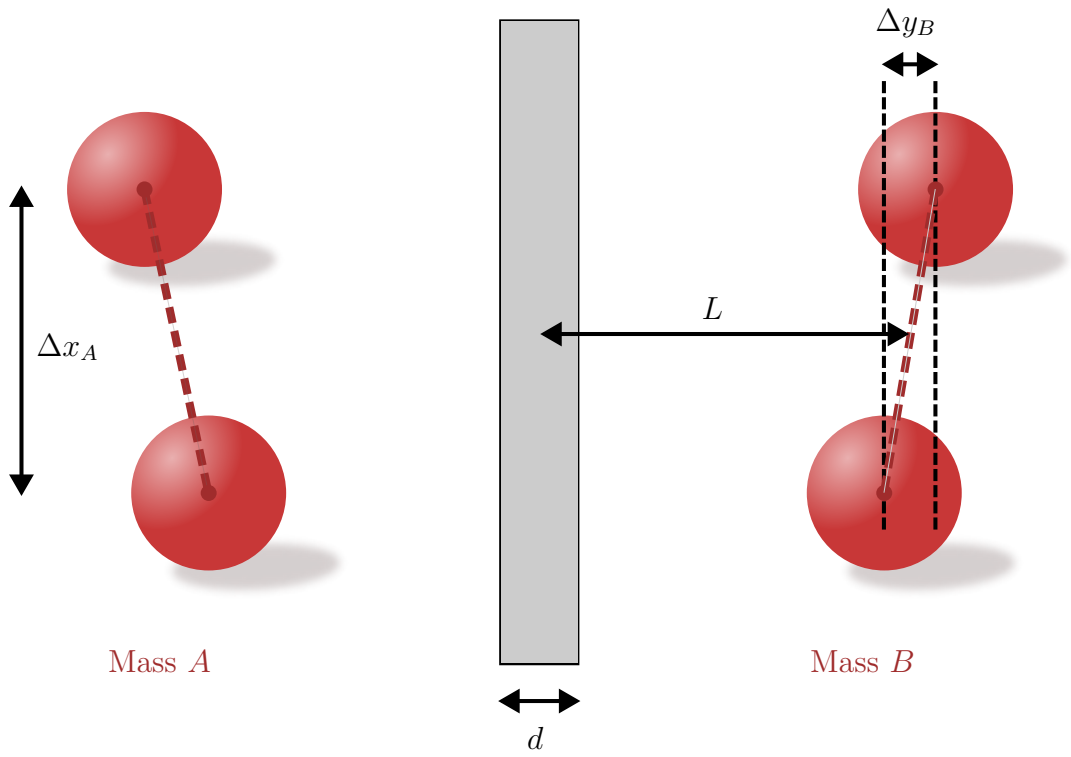

Figure 5.1: My problem

5.1 Orientation

E_N depending on the orientation:

$$E_N = \log_2 \left\{ 1 + \left| \sin\left(\frac{GM_A M_B t}{\hbar} \frac{\Delta x_A \Delta x_B}{8L^3} \left[\sin\alpha \sin\beta - \frac{1}{2}\cos\alpha\cos\beta \right] \right) \right| \right\} \tag{5.1}$$

Time till the maximum entanglement ($E_N = 1$):

$$t_{\max} = \frac{8\pi L^3 \hbar}{2GM_A M_B \Delta x_A \Delta x_B} \left| \sin\alpha \sin\beta - \frac{1}{2}\cos\alpha\cos\beta \right|^{-1} \tag{5.2}$$

with a global minimum for $\alpha, \beta \in [0, \pi]$ for the orthogonal orientation with $\alpha = \beta = \pi/2$. Here, the time till the maximum entanglement is given by

$$t_{\max} = \frac{4\pi\hbar L^3}{GM_A M_B \Delta x_A \Delta x_B} \simeq 129\,\mathrm{mn} \tag{5.3}$$

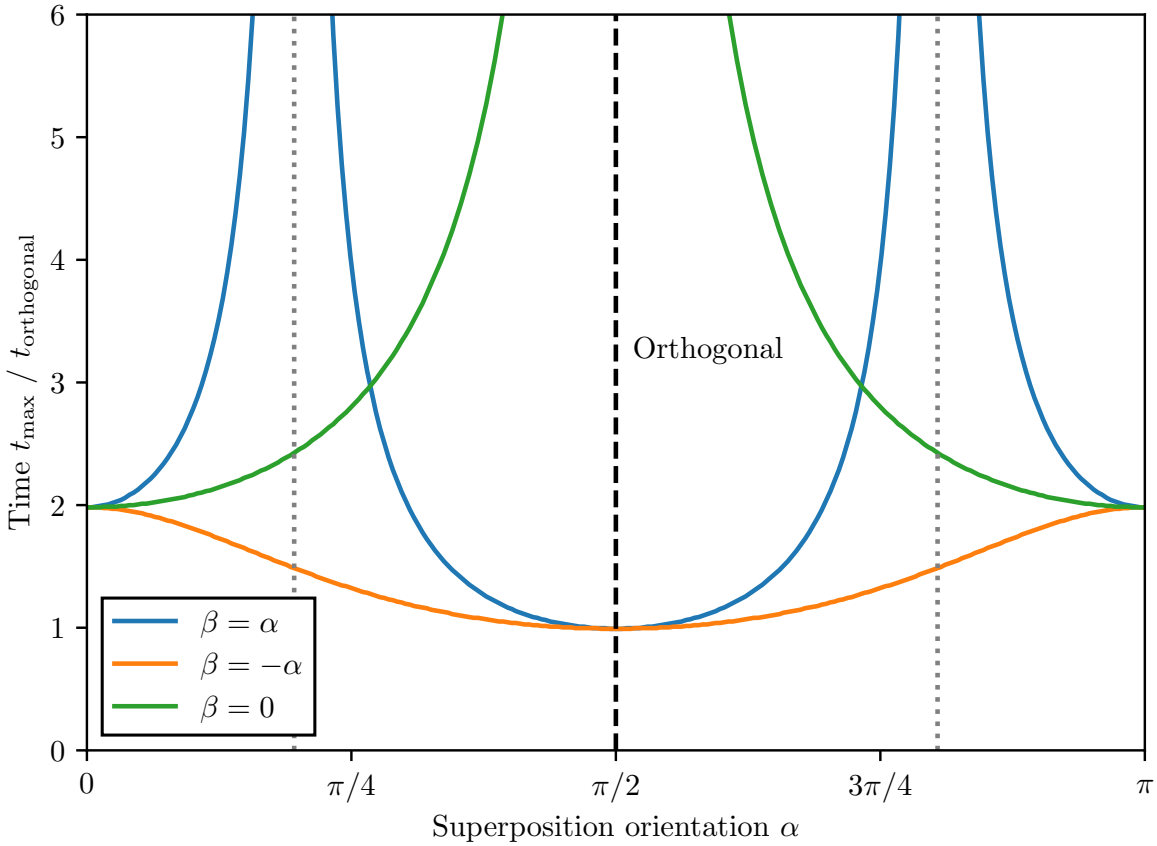

Figure 5.2: ...

Bibliography

[1] S. Bose, A. Mazumdar, G. W. Morley, H. Ulbricht, M. Toroš, M. Paternostro, A. Geraci, P. Barker, M. S. Kim, and G. Milburn, "A Spin Entanglement Witness for Quantum Gravity", Phys. Rev. Lett. **119**, 240401 (2017) 10.1103/physrevlett.119.240401, arXiv:1707.06050.

[2] L. Lami, J. S. Pedernales, and M. B. Plenio, "Testing the quantum nature of gravity without entanglement", Phys. Rev. X **14**, 021022 (2023) 10.1103/physrevx.14.021022, arXiv:2302.03075.

[3] R. Horodecki, P. Horodecki, M. Horodecki, and K. Horodecki, "Quantum entanglement", Rev. Mod. Phys. **81**, 865–942 (2007) 10.1103/revmodphys.81.865, arXiv:quant-ph/0702225.

[4] M. B. Plenio and S. Virmani, "An introduction to entanglement measures", Quantum Information & Computation **7**, 1–51 (2005), arXiv:quant-ph/0504163.

[5] J. S. Pedernales and M. B. Plenio, "On the origin of force sensitivity in tests of quantum gravity with delocalised mechanical systems", Contemporary Physics **64**, 147–163 (2023) 10.1080/00107514.2023.2286074, arXiv:2311.04745.

[6] D. Carney, P. C. E. Stamp, and J. M. Taylor, "Tabletop experiments for quantum gravity: a user's manual", Classical and Quantum Gravity **36**, 034001 (2018) 10.1088/1361-6382/aaf9ca, arXiv:1807.11494.

[7] M. Christodoulou, A. Di Biagio, M. Aspelmeyer, Č. Brukner, C. Rovelli, and R. Howl, "Locally mediated entanglement in linearised quantum gravity", Physical Review Letters **130**, 100202 (2022) 10.1103/physrevlett.130.100202, arXiv:2202.03368.

[8] T. Westphal, H. Hepach, J. Pfaff, and M. Aspelmeyer, "Measurement of Gravitational Coupling between Millimeter-Sized Masses", Nature **591**, 225–228 (2021) 10.1038/s41586-021-03250-7, arXiv:2009.09546.

[9] H. B. G. Casimir, "On the attraction between two perfectly conducting plates", Proc. Kon. Ned. Akad. Wet. **51**, 793 (1948).

[10] H. B. G. Casimir and D. Polder, "The Influence of Retardation on the London-van der Waals Forces", Physical Review **73**, 360–372 (1948) 10.1103/physrev.73.360.

[11] L. Gurvits, "Classical deterministic complexity of Edmonds' problem and Quantum Entanglement", in Proceedings of the thirty-fifth annual acm symposium on theory of computing, Vol. 4, STOC03 (June 2003), pages 10–19, 10.1145/780542.780545, arXiv:quant-ph/0303055.

[12] M. Plenio, "Logarithmic negativity: a full entanglement monotone that is not convex.", Physical Review Letters **95**, 090503 (2005) 10.1103/PhysRevLett.95.090503, arXiv:quant-ph/0505071.

[13] G. Vidal and R. F. Werner, "A computable measure of entanglement", Phys. Rev. A **65**, 032314 (2001) 10.1103/physreva.65.032314, arXiv:quant-ph/0102117.

[14] T. W. van de Kamp, R. J. Marshman, S. Bose, and A. Mazumdar, "Quantum Gravity Witness via Entanglement of Masses: Casimir Screening", Phys. Rev. A **102**, 062807 (2020) 10.1103/physreva.102.062807, arXiv:2006.06931.

[15] M. Hartmann, "Casimir effect in the plane-spheregeometry: Beyond the proximityforce approximation", PhD thesis (Universität Augsburg, July 2018).

[16] T. Emig, "Fluctuation induced quantum interactions between compact objects and a plane mirror", Journal of Statistical Mechanics: Theory and Experiment **2008**, P04007 (2007) 10.1088/1742-5468/2008/04/p04007, arXiv:0712.2199.

[17] A. Bulgac, P. Magierski, and A. Wirzba, "Scalar Casimir effect between Dirichlet spheres or a plate and a sphere", Physical Review D **73**, 025007 (2006) 10.1103/physrevd.73.025007.

[18] D. J. Griffiths, ***Elektrodynamik, Eine Einführung***, edited by U. Schollwöck, 4th edition (Pearson, Hallbergmoos, 2018), 1711 pages.

[19] A. Canaguier-Durand, R. Guérout, P. A. M. Neto, A. Lambrecht, and S. Reynaud, "The Casimir effect in the sphere-plane geometry", International Journal of Modern Physics Conference Series **14**, 250–259 (2012) 10.1142/s2010194512007374, arXiv:1202.3272.

[20] M. A. Nielsen and I. L. Chuang, ***Quantum computation and quantum information***, 10th anniversary ed. (Cambridge University Press, Cambridge, 2010), 1676 pages.

[21] J. S. Pedernales, G. W. Morley, and M. B. Plenio, "Motional Dynamical Decoupling for Matter-Wave Interferometry", Phy. Rev. Lett. **125**, 023602 (2019) 10.1103/physrevlett.125.023602, arXiv:1906.00835.

[22] G. A. E. Vandenbosch, "The basic concepts determining electromagnetic shielding", American Journal of Physics **90**, 672–681 (2022) 10.1119/5.0087295.

[23] L. H. Ford, "Casimir Force between a Dielectric Sphere and a Wall: A Model for Amplification of Vacuum Fluctuations", Phys. Rev. A **58**, 4279–4286 (1998) 10.1103/physreva.58.4279, arXiv:quant-ph/9804055.

[24] I. G. Pirozhenko and M. Bordag, "On the Casimir repulsion in sphere-plate geometry", Physical Review D **87**, 085031 (2013) 10.1103/physrevd.87.085031, arXiv:1302.5290.

[25] T. Emig, N. Graham, R. L. Jaffe, and M. Kardar, "Casimir forces between arbitrary compact objects", Phys. Rev. Lett. **99**, 170403 (2007) 10.1103/physrevlett.99.170403, arXiv:0707.1862.

[26] E. M. Lifshitz, "The theory of molecular attractive forces between solids", Sov. Phys. JETP **2**, 73–83 (1956) 10.1016/b978-0-08-036364-6.50031-4.

A TITLE TO BE DONE

A.1 Evolution under a gravitational Hamiltonian

In this section the time evolution of a system under Hamiltonian eq. (2.3) is calculated a) using the gravitational interaction $\hat{H}_G$ as a perturbation b) using an exact time evolution of coherent states.

A.1.1 Using time dependent perturbation theory

A general biparty Fock state $|\psi_0\rangle = |kl\rangle$ with $k, l \in \mathbb{N}_0$ can be evolved in time under a Hamiltonian eq. (2.3) treating the gravitational interaction $H_G = -\hbar g(\hat{a}_1\hat{a}_2^\dagger + \hat{a}_1^\dagger\hat{a}_2)$ as a perturbation. The resulting state $|\psi(t)\rangle$ after some time t is in the most general form given as

$$|\psi(t)\rangle = \sum_{i,j\geq 0} c_{i,j}(t)\,|i,j\rangle \tag{A.1}$$

where the coefficients $c_{i,j}(t)$ are given by first order perturbation theory as

$$c_{i,j}(t) = c_{i,j}(t=0) - \frac{i}{\hbar}\int_0^t \mathrm{d}t'\,\langle ij|\,\hat{H}_G\,|kl\rangle\,e^{-i(E_{kl}-E_{ij})t'/\hbar}. \tag{A.2}$$

The exponent is given by the energy of the appropriate Fock states $E_{kl} - E_{ij} = \hbar\omega(k + l - (i + j))$ and the matrix element in the integrand can be calculated to

$$\langle ij|\,\hat{H}_G\,|kl\rangle = \begin{cases} -\hbar g & \text{if } i = k \pm 1 \text{ and } j = l \mp 1 \\ 0 & \text{otherwise} \end{cases}. \tag{A.3}$$

The coefficients for $t = 0$ are trivially given from the initial state as

$$c_{i,j}(t=0) = \begin{cases} 1 & \text{for } i,j = k,l \\ 0 & \text{otherwise} \end{cases}. \tag{A.4}$$

For the non-zero states the energies in the exponent equate to zero and the evolved state is given by (up to a normalization)

$$|\psi(t)\rangle = |kl\rangle - igt\,|k-1, l+1\rangle - igt\,|k+1, l-1\rangle + \mathcal{O}(g^2). \tag{A.5}$$

The result eq. (2.5) is represented by eq. (A.5) for the case of $k = 1$ and $l = 0$.

A.1.2 Using an exact time evolution

The Hamiltonian eq. (2.3) can be rewritten using symmetric and antisymmetric normal modes

$$\hat{a}_\pm = \frac{1}{\sqrt{2}}\left(\hat{a}_1 \pm \hat{a}_2\right) \tag{A.6}$$

in the form of

$$\hat{H} = \hbar\omega_+ \hat{a}_+^\dagger \hat{a}_+ + \hbar\omega_- \hat{a}_-^\dagger \hat{a}_-, \quad \omega_\pm = \omega \pm (-g) \tag{A.7}$$

The initial state consisting of two coherent oscillator states is in the new modes given by

$$|\psi(t)\rangle = |\alpha\rangle_1 |\beta\rangle_2 = \left|\frac{1}{\sqrt{2}}(\alpha+\beta)\right\rangle_+ \left|\frac{1}{\sqrt{2}}(\alpha-\beta)\right\rangle_- \tag{A.8}$$

A general coherent state $|\gamma\rangle$ evolves in time under an Hamiltonian $\hat{H} = \hbar\omega\hat{a}^\dagger\hat{a}$ like $|\gamma(t)\rangle = |e^{-i\omega t}\gamma\rangle$ which can be used to evolve the state in eq. (A.8):

$$|\psi(t)\rangle = \left|\frac{1}{\sqrt{2}} e^{-i\omega_+ t}(\alpha+\beta)\right\rangle_+ \left|\frac{1}{\sqrt{2}} e^{-i\omega_- t}(\alpha-\beta)\right\rangle_- \tag{A.9}$$

$$= \left|e^{-i\omega t}\left(\alpha\cos gt - \beta\sin gt\right)\right\rangle_1 \left|e^{-i\omega t}\left(-\alpha\sin gt + \beta\cos gt\right)\right\rangle_2, \tag{A.10}$$

where in the last line the back-transformation from the $\pm$-modes (A.8) was used.

A.2 Exemplary calculation of E_N

In this section, the logarithmic negativity E_N eq. (2.20) is exemplary calculated for the state eq. (2.13). The density matrix of this system is given by

$$\rho(t) = |\psi(t)\rangle\langle\psi(t)| = \frac{1}{4}\begin{pmatrix} 1 & e^{i\Delta\phi} & e^{i\Delta\phi} & 1 \\ e^{-i\Delta\phi} & 1 & 1 & e^{-i\Delta\phi} \\ e^{-i\Delta\phi} & 1 & 1 & e^{-i\Delta\phi} \\ 1 & e^{i\Delta\phi} & e^{i\Delta\phi} & 1 \end{pmatrix}. \tag{A.11}$$

Consequently, the partially transposed density ρ^{Γ_B} is given by

$$\rho^{\Gamma_B}(t) = \frac{1}{4}\begin{pmatrix} 1 & e^{-i\Delta\phi} & e^{i\Delta\phi} & 1 \\ e^{i\Delta\phi} & 1 & 1 & e^{-i\Delta\phi} \\ e^{-i\Delta\phi} & 1 & 1 & e^{i\Delta\phi} \\ 1 & e^{i\Delta\phi} & e^{-i\Delta\phi} & 1 \end{pmatrix}. \tag{A.12}$$

The eigenvalues where calculated using `Mathematica` and equate to

$$\left\{\sin^2\left(\frac{\Delta\phi}{2}\right), \cos^2\left(\frac{\Delta\phi}{2}\right), \frac{\sin\Delta\phi}{2}, -\frac{\sin\Delta\phi}{2}\right\}$$

According to lemma 2.1, $\left\|\rho^{\Gamma_B}\right\|_1$ is given by the sum of the absolute eigenvalues, which is equal to $1 + |\sin \Delta\phi|$. The negativity as the absolute sum of all negative eigenvalues (demonstrated in proposition 2.3) equates to $\mathcal{N} = |\sin \Delta\phi| /2$. Both methods result in a logarithmic negativity of $E_N = \log_2(1 + |\sin \Delta\phi|)$.